SUPPLEMENTARY INFORMATION

Supplementary figure 1. Setup of the light sheet microscope ultramicroscope.
Schematic representations of (**A**) the excitation pathway of the collimated beam and (**B**) the detection pathway of the fluorescence signal.
(A) The collimated beam of a supercontinuum white light laser (465 – 2400 nm; repetition rate 80 MHz) passes a blocking filter (BF) to inhibit the IR part (750 - 2400 nm) of the spectrum. The subsequent beam path includes a circular, variable, metallic neutral density filter wheel (ND) to allow continuous adjustment of the excitation power and a band-pass filter (BP) to select a specific part of the spectrum for excitation. A telescope (L_1, L_2) is used to enlarge the beam diameter from ~1 to 10 mm. The sample is illuminated sequentially from opposing sides by a flip-mirror (FM). Both beam pathways feature identical length and optical elements: Routing mirrors (M) guide the laser beam through a vertically variable slit (AP) that allows adjustment of the numerical aperture (NA) of the excitation beam. Alteration of the NA changes the light sheet thickness, the depth of focus and accordingly the usable length of the field of view. The full NA corresponds to a light sheet thickness of 4.5 µm in the centre of the field of view at 488nm excitation wavelength. A galvanometric scanner (SC) located in the back focal plane of the illumination objective lens (OL) rasters the laser beam in y-direction across the field of view to form the light sheet. Compared to light sheet generation through cylindrical lenses, this method efficiently prevents shadowing that causes dark stripes within the images. The sample chamber contains benzyl alcohol and benzyl benzoate (BABB). **(B)** Emitted fluorescence is collected through a macro objective (OL) (2x magnification; 0.5 NA) with a dipping cap in front. A filter wheel (FW) equipped with different emission band-pass filters allows sequential acquisition of signals from various fluorophores before the tube lens (TL) focuses the light onto a CCD chip.

Supplementary figure 2. Embryonic vasculature at different developmental stages.
(**A-M**) 3D reconstruction of wildtype embryos, wholemount-immunostained for the indicated proteins at E9.75 and 10.5. (**I-M**) represents higher magnification images of the jugular-thoracic region of embryo showed in (**D-H**). Colors as noted in the labeling laterally to each panel.
(**A-C**)Unlike PECAM-1 (**Fig. 1 A**), Endomucin strongly identified capillary structures and venous vessels. Compared to VEGFR-3 (**B**), Endomucin showed a similar but not identical expression pattern at E9.75. (**D-M**) Using Endomucin as a surrogate marker for venous vessels and PECAM-1 for arterial vessels, venous and arterial vasculature can be distinguished. In combination with Prox1 staining the emerging lymphatic endothelial cells can be identified. (**I-M**) Zoom into jugular-thoracic region. Scale bars = 100 µm.

Supplementary figure 3. A side branch of the subclavian artery separates highly Prox1+ cells at the interface between pTD and CV.

Shown are 3D reconstructions of optically sectioned wildtype embryo wholemounts at E11.5. Detected antigens and the corresponding colors are noted above each panel, sagittal view.

(**A**) High PECAM-1 expression delineates the arterial vasculature. (**B, C**) The interface between the nascent lymphatic vasculature and the CV is marked by high Prox1 expression. An artery (arrowhead) stereotypically located between the highly Prox1+ tandem connections of CV and pTD is branching from the subclavian artery. BA, basilar artery; CA, carotid artery, DA, dorsal aorta; PAA, pharyngeal arch artery; SA, subclavian artery; VA, vertebral artery. Corresponding video (**Suppl. video 1**). Scale bars = 100 µm.

Supplementary figure 4. Podoplanin is not expressed on Prox1+ cells of the cardinal vein and iLECs, but starting at E11.0 on the pTD and on sLECs.

Shown are immunostainings of cryosections. The detected antigens and the corresponding colors are noted above each panel.

(A, B) At E10.0 Podoplanin expression is absent on all vascular structures, including the CV (arrows) and iLECs (arrowheads), while the neural tube (NT) stains strongly positive for podoplanin. **(C, D)** Podoplanin expression is initiated at E11.0 on LECs (arrowheads) outside the CV and is strongly upregulated in all lymphatic structures over the next 24 hours (asterisk) **(E, F)**. In contrast, Prox1+ ECs in the CV (B, C, D arrows) remain Podoplanin negative. Scale bars = 100 µm.

Supplementary figure 5. Antidromic expression pattern of Lyve-1 and Nrp2 on migrating LECs and lumenized lymphatic structures.

Shown are immunostainings of cryosections. The detected antigens and the corresponding colors are noted above each panel.

(**A-F**) Lyve-1 and Nrp2 show largely antidromic expression patterns. Lyve-1 was found strongly expressed on lumenized, more mature lymphatic structures (arrowhead) like the pTD, while the superficial lymphatic front (arrow) showed only low expression. In contrast, Nrp2 was highly upregulated in migrating iLECs and sLECs (arrows), but only moderately expressed in the pTD (arrowheads). Additionally, both proteins were found in the Prox1+ cells of the CV. Scale bars = 100 µm. **(G)** VE-Cadherin staining of Prox1+ cells showing non-luminized iLECs. Scale bars = 100 µm.

Supplementary figure 6. Expression pattern of different markers on LECs.

(**A-T**) Shown are immunostainings of cryosections. The detected antigens and the corresponding colors are noted above each panel.

(**A-D**) Integrin α6 expression was detected on the CV, pTD and on sLECs (arrowheads) at E11.0 and E11.5. (**E-H**) At 11.0, Netrin-4 was not expressed on iLECs outside the CV. At E11.5, Netrin-4 was detected on lumenized structures like the pTD, but was absent from sLECs (arrowheads). At the same time, blood capillaries (arrows) were strongly positive for Netrin-4 expression. (**I-L**) At E10.5 the CV as well as the iLECs are strongly positive for VEGFR-2. Expression is downregulated in the CV at E11.5, while LECs still express higher levels of VEGFR-2. (**M-P**) Integrin β1 is expressed on all LECs at E10.5 and E11.5 (**Q-T**) Integrin α9 is absent on LECs. At later stages the region of the lymphovenous valve stains positive for Integrin α9 (arrowhead). Scale bars = 100 µm.

Supplementary figure 7. Unc5B is expressed on migrating and lumenized Prox1+ LECs outside the CV.

Immunostainings of histological cryosections **(A-D)** and wholemount preparations **(E-G)**, sagittal view. The detected antigens and the corresponding colors are noted above each panel.

(**A-D**) At E11.0, Unc5B was readily detected on Prox1+ LECs outside the CV (arrowheads), while Unc5B expression on the endothelium of the CV was weak (arrows). **(E-G)** Wholemount staining for Unc5B and Prox1 outlined the newly formed lymphatic architecture comprised of the pTD, PLLV and dorsal superficial lymphatics. Unc5B was absent from Prox1+ cells of the developing lymphovenous valve (arrow). Dashed line, CV; cranial, left; caudal, right; scale bars = 100 µm.

Supplementary figure 8. EdU staining demonstrates little proliferation of Prox+ cells in the CV and pTD, but stronger proliferation in sLECs at E11.5.

Shown are 5-ethynyl-2′-deoxyuridine (EdU)-labeling and immunostainings of cryosections to detect DNA synthesis in proliferating cells at different developmental stages. Colors corresponding to the detected antigens and EdU incorporation are noted above each panel.

(**A-D**) At all stages analyzed (E9.5 - E11.5) EdU incorporation into Prox1+ cells (arrowhead), including the pTD and Prox1+ cells of the CV, was exceedingly rare. At E11.5 sLECs appeared to incorporate EdU more frequently (no EdU incorporation, arrowhead; EdU incorporation, arrow). Scale bars = 100 µm.

Supplementary figure 9. VEGFR-3 gene dosis controls proper formation of pTD and sLEC patterning at E12.5.

(**A-D, F-I**) Sagittal optical sections of *Vegfr3*+/- (**A-D**) and *Vegfr3*+/+ (**F-I**) embryos at E12.5, wholemount-immunostained for the indicated proteins. Colors as noted in the labeling above each panel. Long-hatched lines denote the position of the CV. Cranial, left; caudal, right.

(**A-D**) In *Vegfr3* heterozygous embryos a reduced number of LEC outside the CV were detectable. Compared to WT littermates (**F-I**), formation of the contact site (asterisk) was unimpaired. In addition to a reduced VEGFR-3 expression level, heterozygous embryos showed mispatterned sLECs and an absence of Y-shaped sLEC structures (arrowheads). The pTD was also affected and appeared to be of a disrupted, non-tubular structure (arrows). (**E+J**) Schematic representation of the lymphatic vasculature at E12.5 in WT and *Vegfr3* heterozygous embryos. Scale bars = 100 µm.

Supplementary figure 10. CCBE1 expression is temporally and spatially tightly restricted to areas adjacent to Prox1+ cells and nascent lymphatic structures.

LacZ wholemount staining of *Ccbe1-LacZ* embryos revealing areas of CCBE1 expression at the indicated time points of embryonic development.

(**A**) At E10.5, CCBE1 expression was predominately detected in the somites and cardiac mesothel (arrow). (**B**) At E11.5, CCBE1 was temporally expressed dorsal to the heart extending in the cranio-caudal direction over the CCV (arrowhead). (**C**) At E12.5, this expression domain rapidly contracted to a small spot at the base of the developing arm. Of note, that underneath this area the primordial lymphovenous valve develops (arrow). Additionally, a second expression domain developed caudally, dorsal to the developing leg.

Supplementary figure 11. In CCBE1-deficient embryos Prox1+ cells form aberrant sprouts but fail to separate from the CV.

(**A, B, D**) 3D reconstructions and (**C, E**) individual planes (optically sectioned) of *Ccbe1-/-* embryos, wholemount-immunostained for the indicated proteins at different developmental stages. Colors as noted in the labeling above.

(**A, D, E**) sagittal view, (**B**) transversal view. In *Ccbe1-/-* embryos displayed prominent atypical, blunt sprouts of Prox1+ cells from the ISV and CV (arrowheads). Additionally, Prox1+ EC in the superficial venous plexus (sVP) formed lumenized sprouts towards the area of the developing PLLV (arrow). (**C**) At E11.5, Prox1 and VEGFR-3 staining was not detectable in the area between PLLV and pTD. Scale bar = 100 µm.

Supplementary video 1. Arterial vasculature and developing lymphatic system in a mouse embryo at E11.5.

Shown is a 3D reconstruction of an optically sectioned wild type embryo at E11.5.

Fluorescence immunostaining for PECAM-1 (red) reveals the arterial vasculature, while Prox1 (green) and VEGFR-3 (blue) delineate the developing lymphatic system. VEGFR-3 is also expressed in venous endothelium. To areas of strongly Prox1 expressing cells at the contact points of pTD and CCV are stereotypically intersected by a transient side branch of the subclavian artery. Structures are also denoted within corresponding images in **suppl. Fig. 3**.

Supplementary video 2. Abnormal sprouts of Prox1+ LECs in CCBE1-deficient embryos at E10.5.

Shown is a 3D reconstruction of an optically sectioned wholemount immunostained *Ccbe1-/-* embryo at E10.5.

Fluorescence immunostaining for endothelial marker PECAM-1 (red, preferentially arterial vessels), VEGFR-3 (blue, venous vessels and developing lymphatics) and the transcription factor Prox1 (green, lymphatic endothelial nuclei) showing atypical, blunt-ending, dilated sprouts comprised of Prox1+ LECs. The sprouts emerge from the CV, ISV and sVP towards the areas corresponding to the developing pTD and PLLV in wildtype embryos. The movie corresponds to **Fig.7 F**.

Supplementary video 3. Prox1+ LECs fail to leave their venous sources in VEGF-C-deficient embryos at E10.75.

Shown is a 3D reconstruction of an optically sectioned wholemount immunostained $Vegfc^{lacZ/lacZ}$ embryo at E10.75.

Fluorescence immunostaining for endothelial marker PECAM-1 (red, preferentially arterial vessels), VEGFR-3 (light blue-grey, venous vessels and developing lymphatics) and the transcription factor Prox1 (green, lymphatic endothelial nuclei) identifies Prox1 expressing cells in the venous vasculature. Due to VEGF-C-deficiency, lymphatic progenitors are trapped within the venous vessels. Besides the CCV and ISVs, Prox1+ cells were also detected in a subpopulation of venous ECs (forming a longitudinal vessel) at the ventral border of the sVP. The movie corresponds to **Fig.8 E,F**

Supplementary Figure 1 (Hägerling & Pollmann et al.)

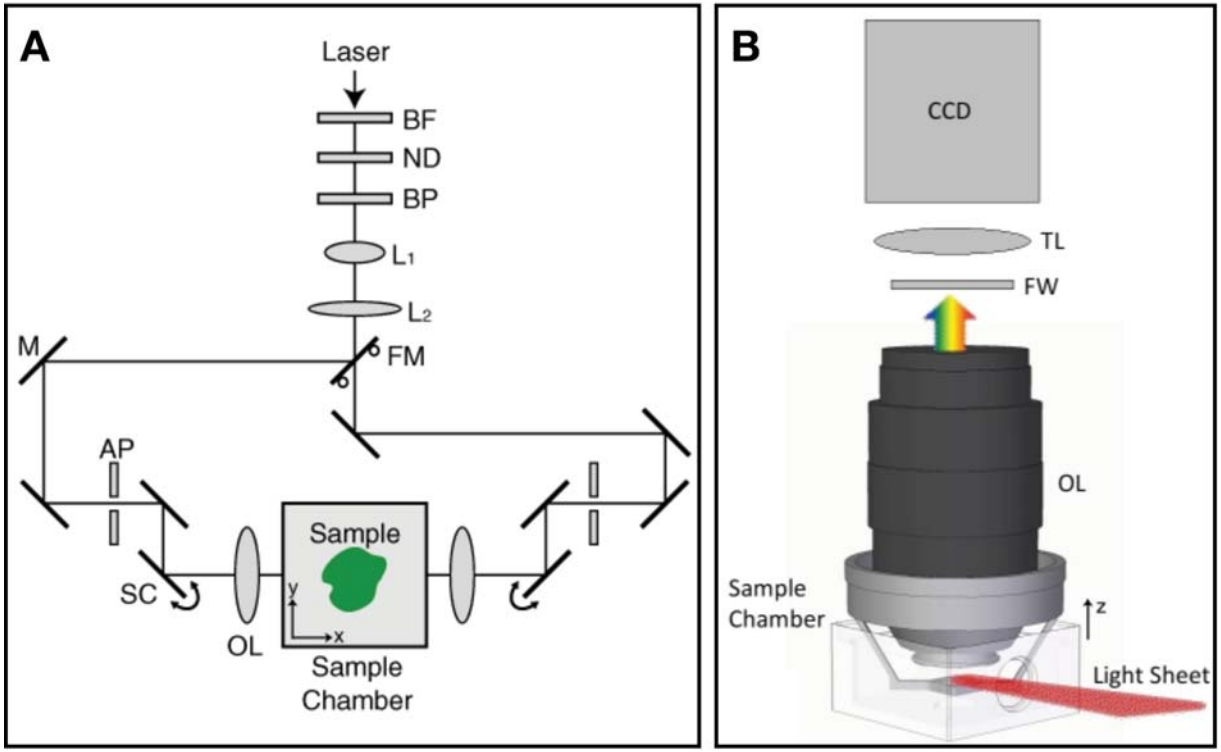

Supplementary Figure 2 (Hägerling & Pollmann et al.)

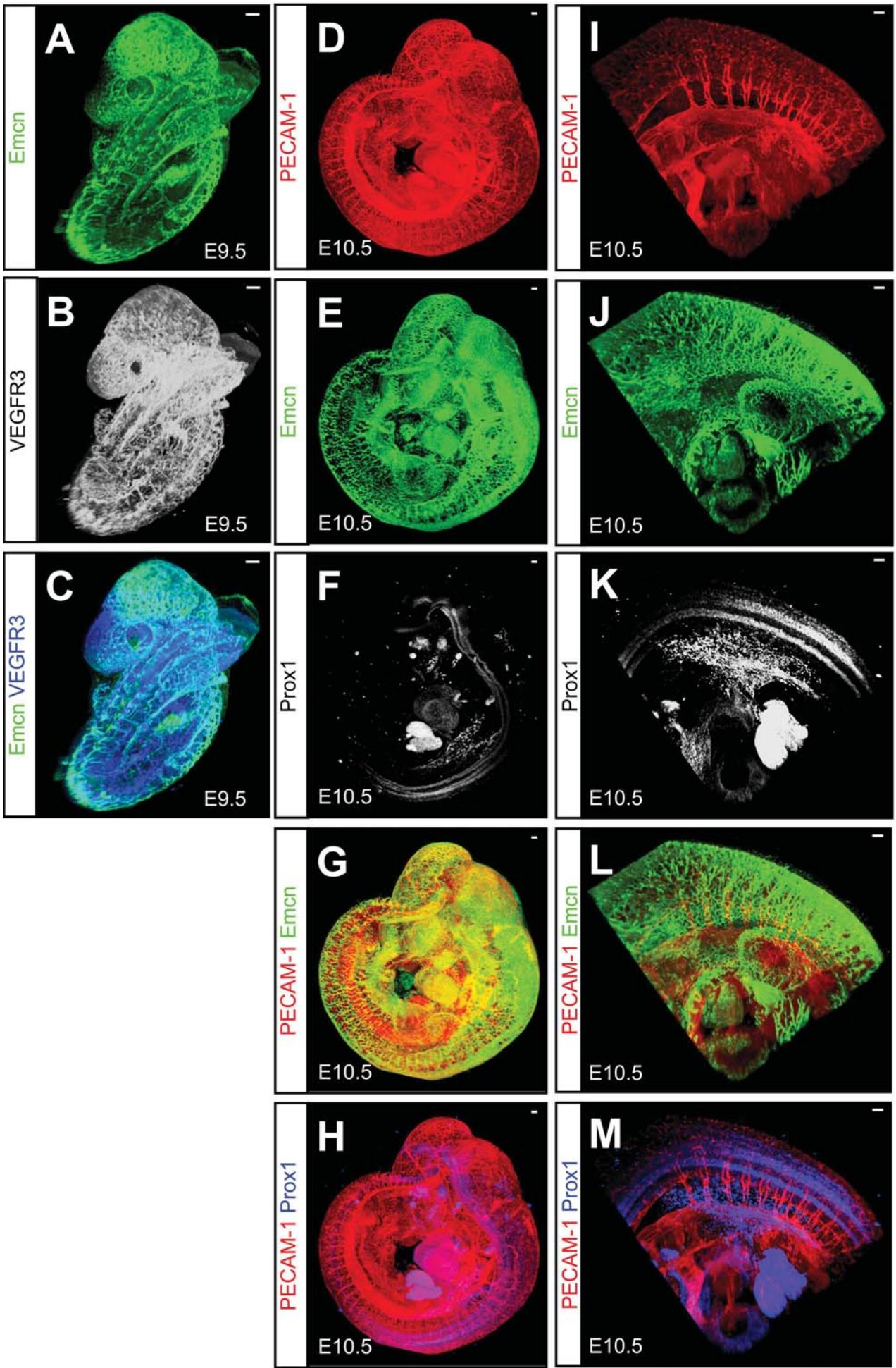

Supplementary Figure 3 (Hägerling & Pollmann et al.)

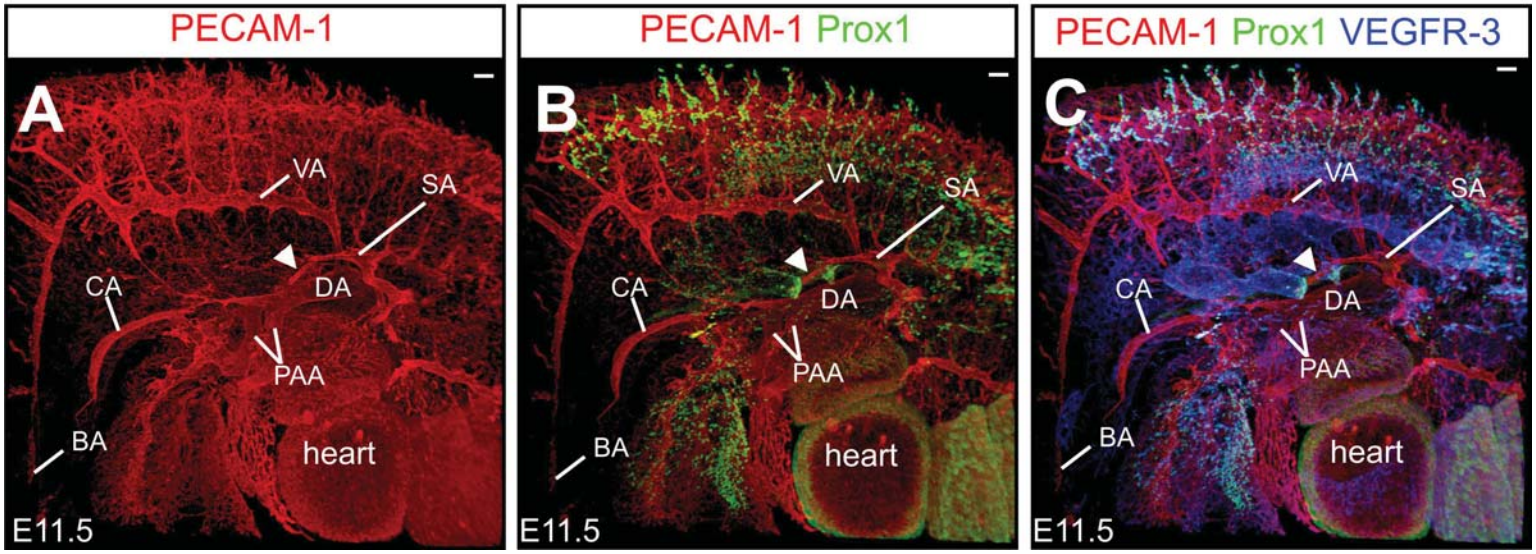

Supplementary Figure 4 (Hägerling & Pollmann et al.)

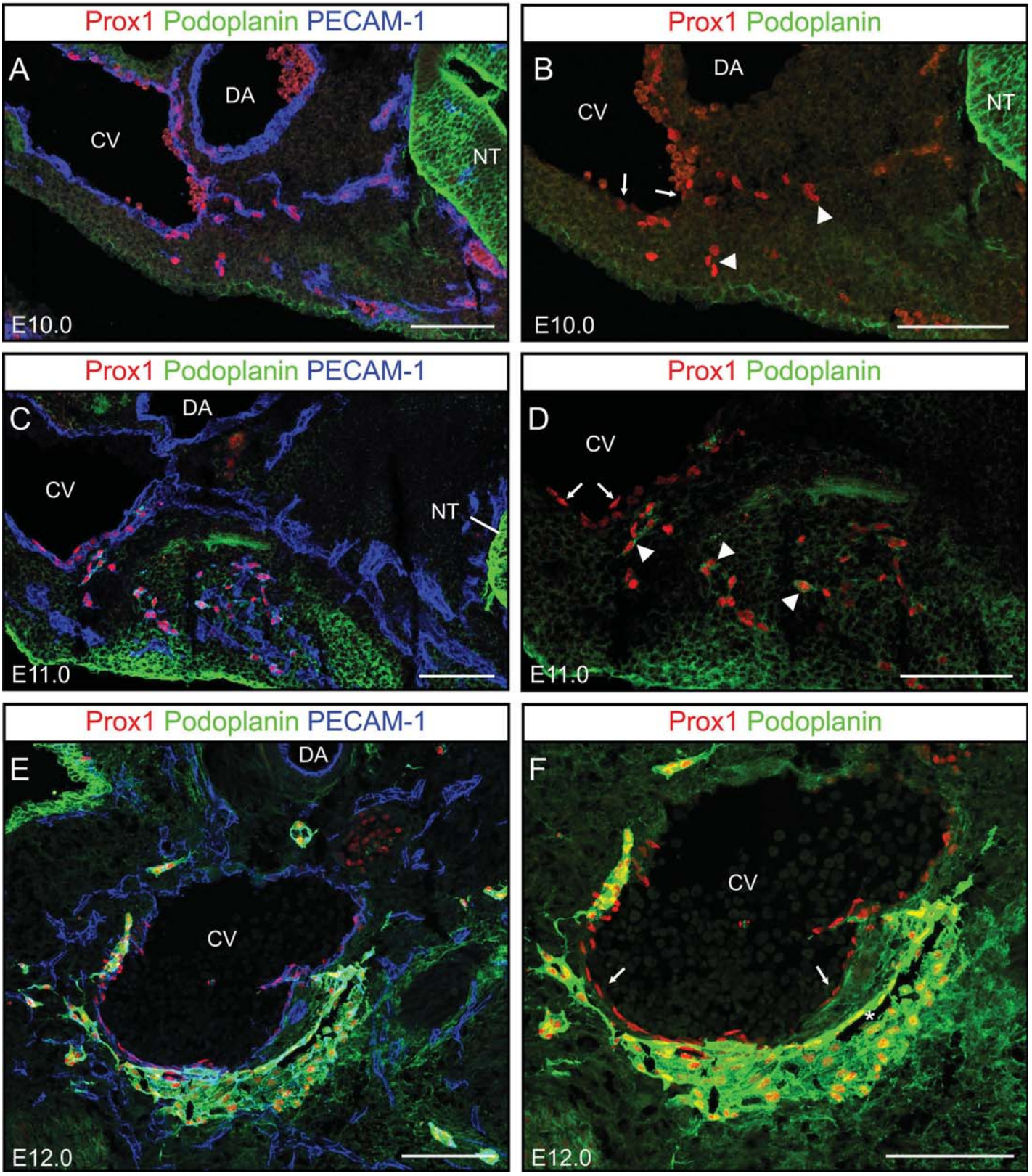

Supplementary Figure 5 (Hägerling & Pollmann et al.)

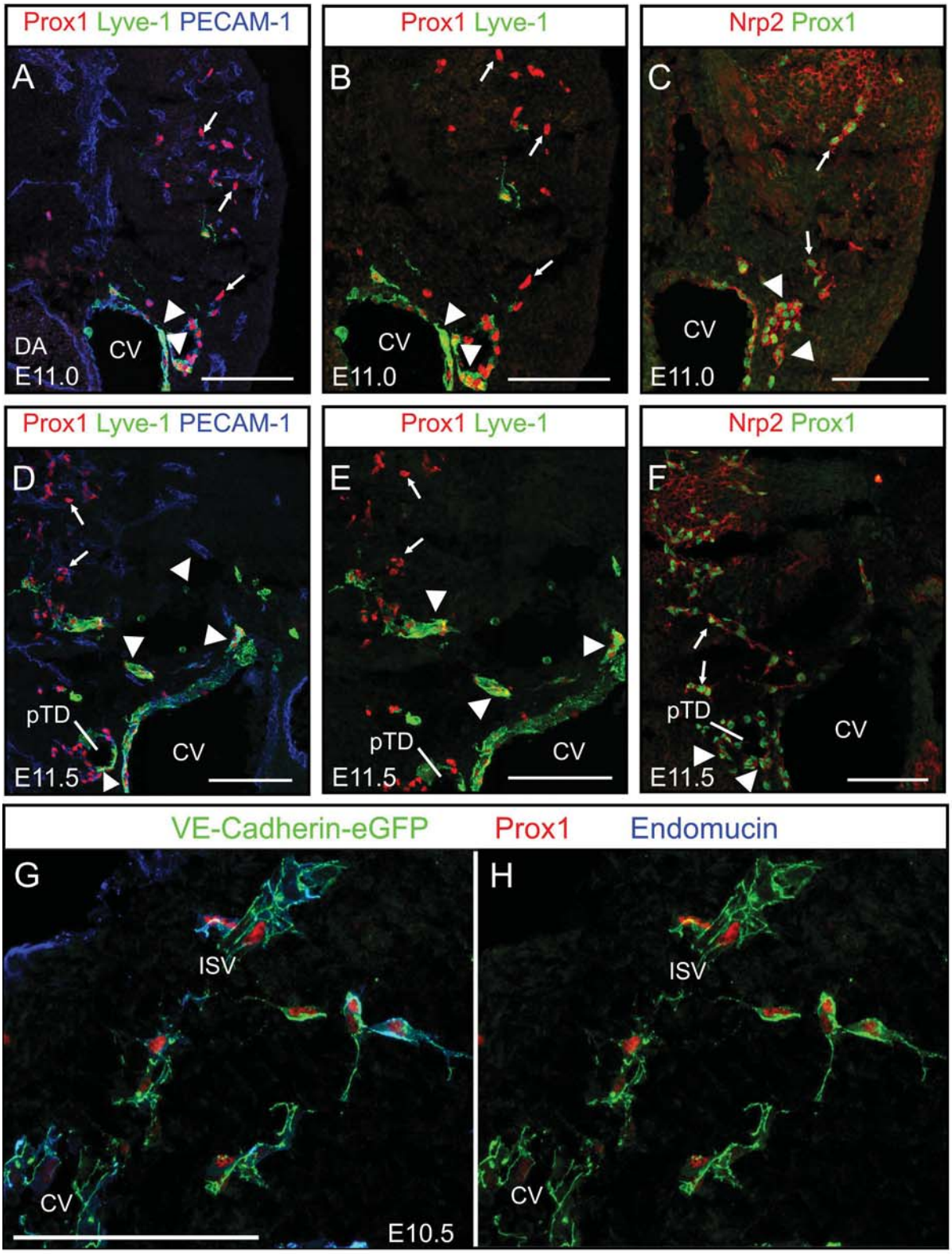

Supplementary Figure 6 (Hägerling & Pollmann et al.)

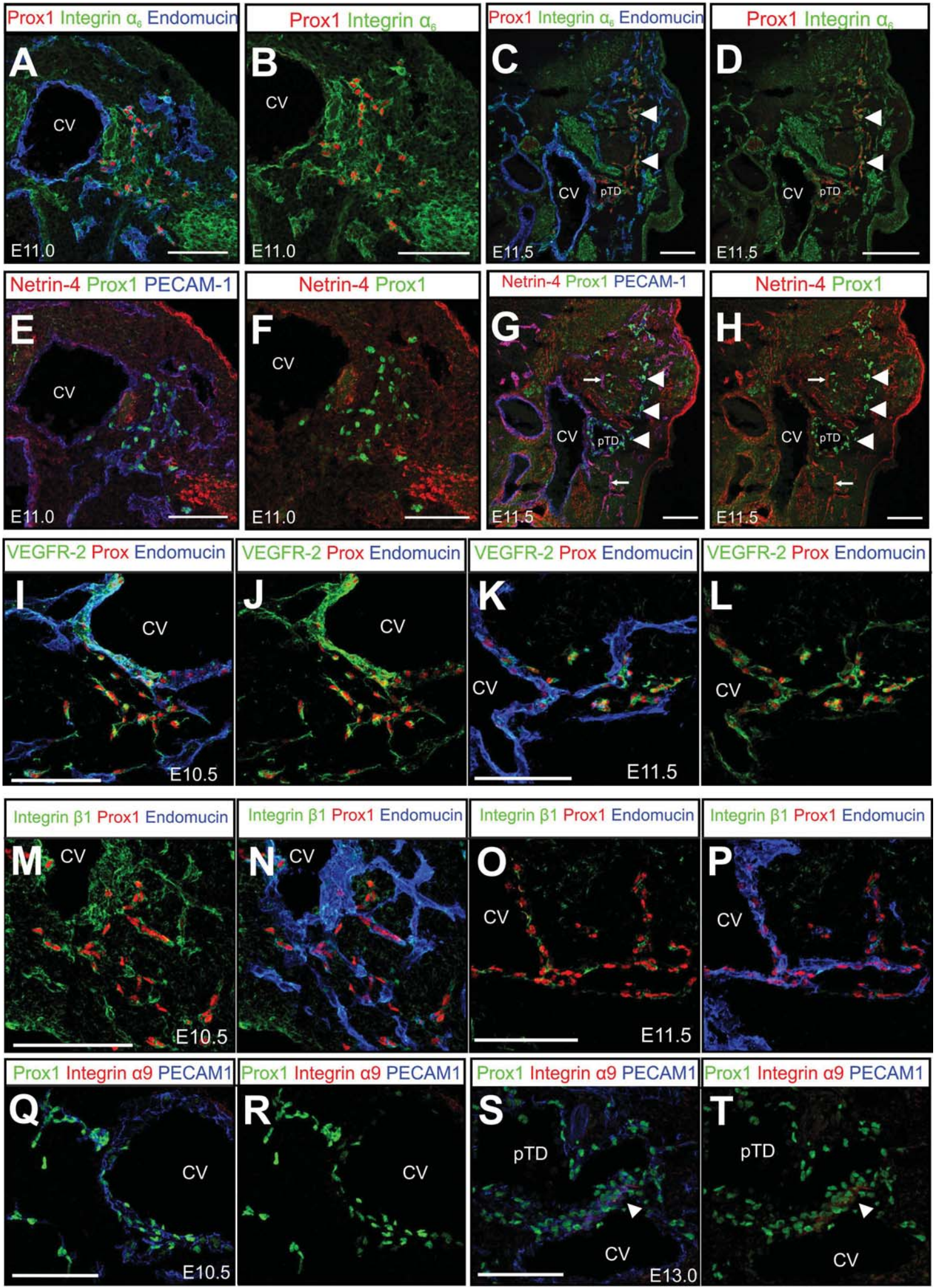

Supplementary Figure 7 (Hägerling & Pollmann et al.)

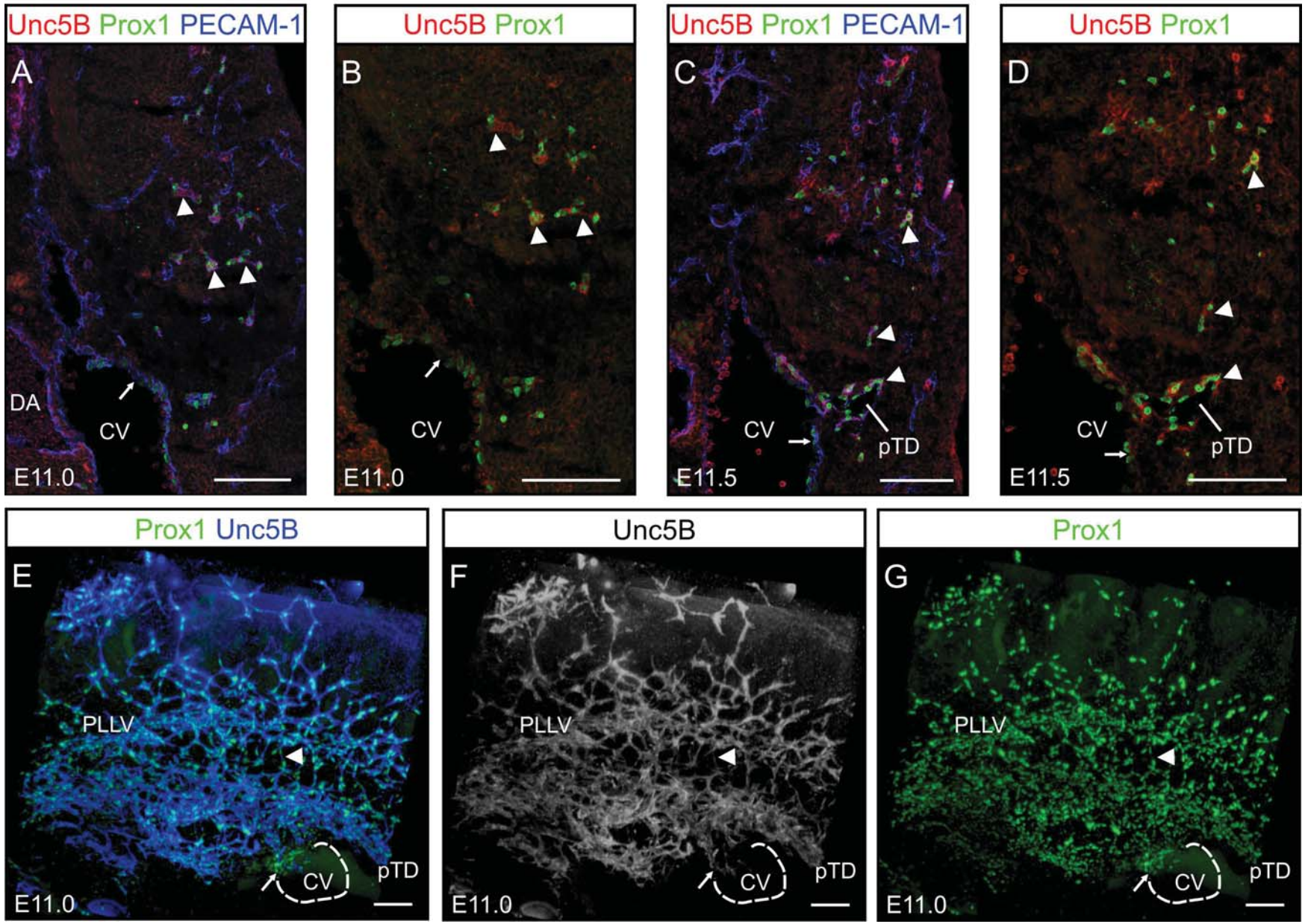

Supplementary Figure 8 (Hägerling & Pollmann et al.)

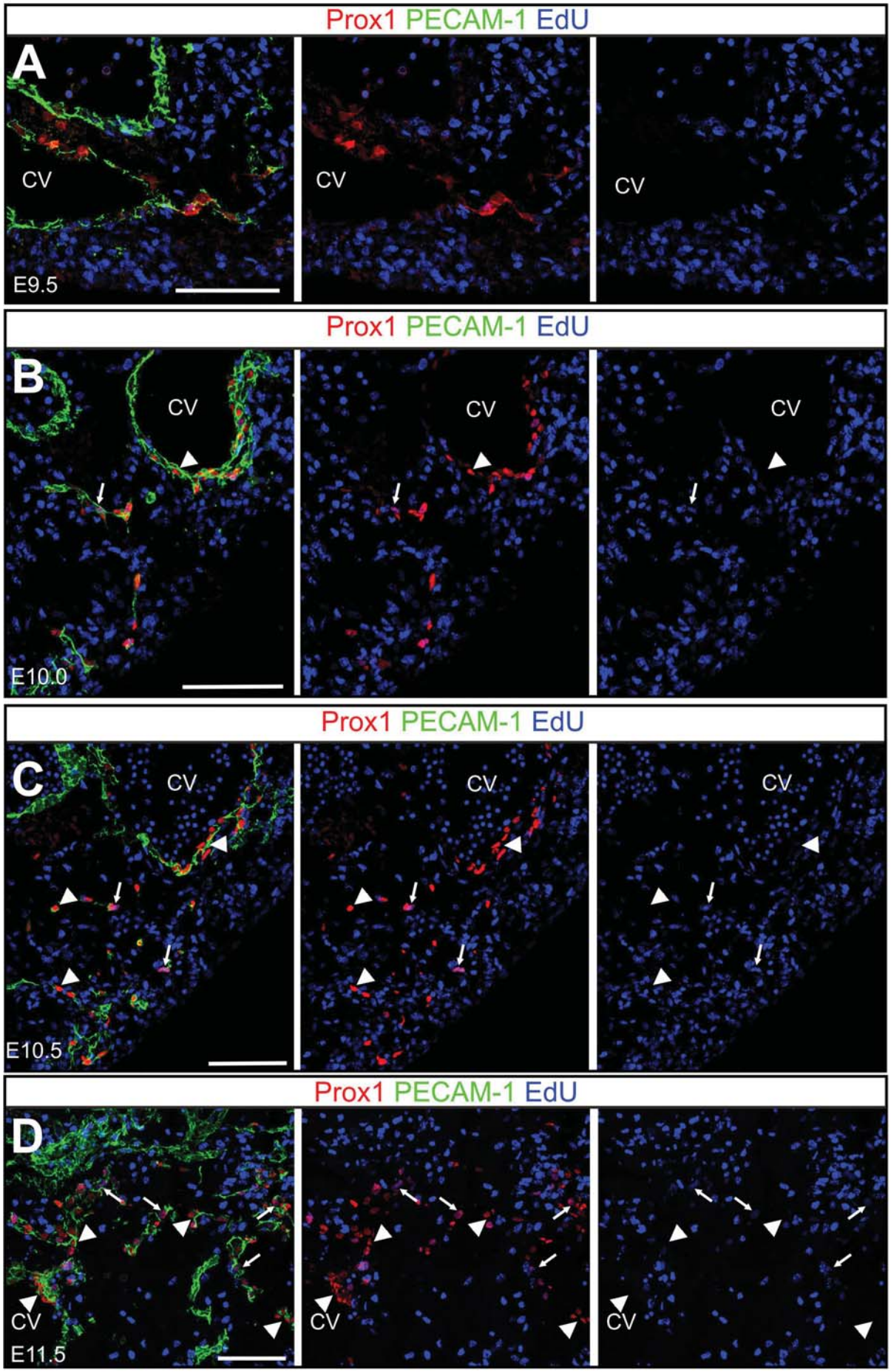

Supplementary Figure 9 (Hägerling & Pollmann et al.)

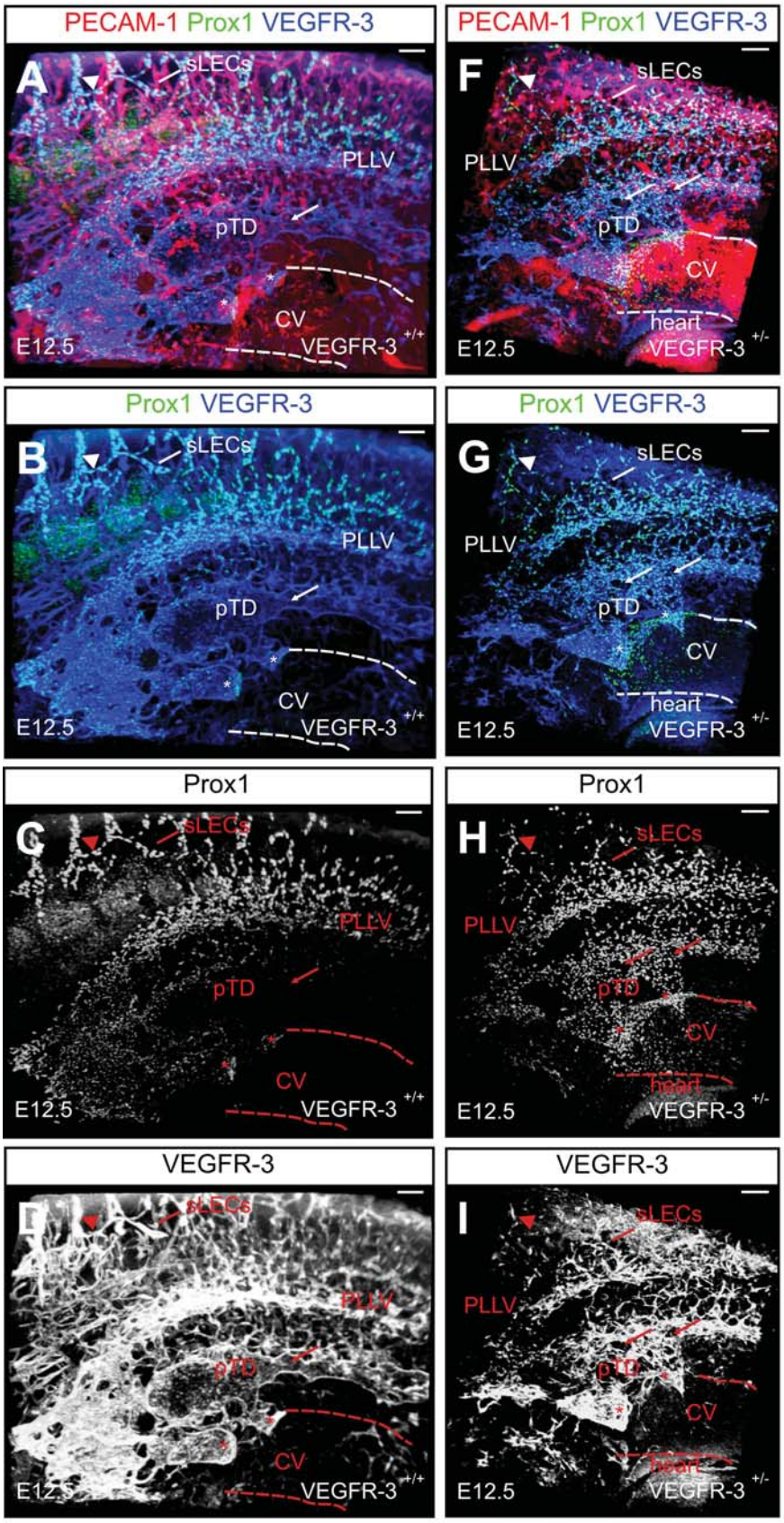

Supplementary Figure 10 (Hägerling & Pollmann et al.)

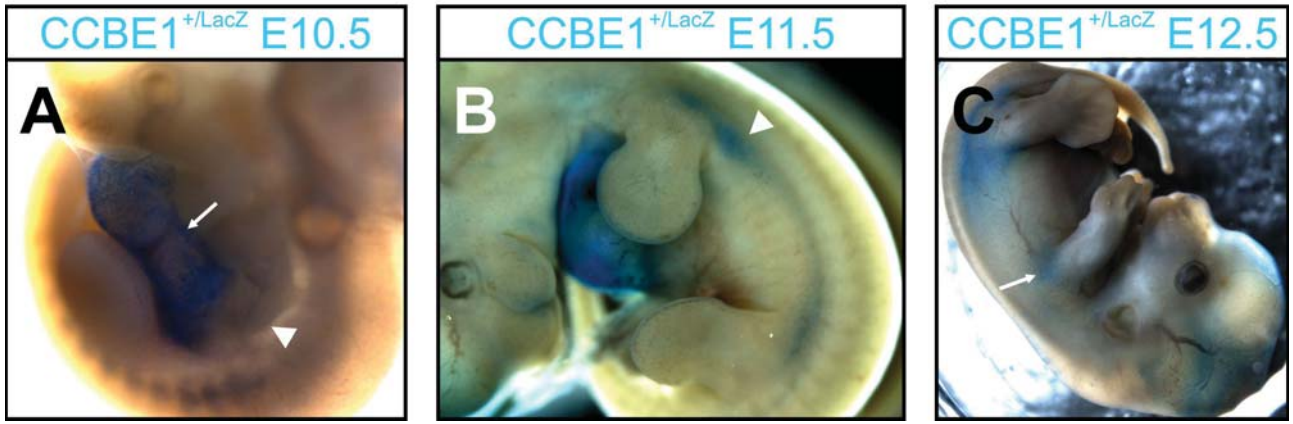

Supplementary Figure 11 (Hägerling & Pollmann et al.)